4b-0048

17WCEE
Sendal, Japan
2020

17th World Conference on Earthquake Engineering, 17WCEE
Sendai, Japan - September 13th to 18th 2020

# COMPARISON OF SEISMIC COMPRESSION PROCEDURE PREDICTIONS: CASE HISTORY FROM JAPAN

R.A. Green<sup>(1)</sup>, Y. Jiang<sup>(2)</sup>

- (1) Professor, Department of Civil and Environmental Engineering, Virginia Tech, rugreen@vt.edu
- (2) Graduate Student, Department of Civil and Environmental Engineering, Virginia Tech, yusheng6@yt.edu

#### Abstract

Seismic compression is the accrual of contractive volumetric strain in unsaturated or partially saturated sandy soils during earthquake shaking and has caused significant distress to overlying and nearby structures, to include the 2007, M<sub>w</sub>6.6 Niigata-ken Chuetsu-oki, Japan earthquake. Of specific interest to this study is the seismic compression that occurred during this event at the Kashiwazaki-Kariwa Nuclear Power Plant (KKNPP) site. What makes this case history of particular value is that the motions at the site were recorded by a free-field downhole array (Service Hall Array, SHA) and the magnitude of the seismic compression was accurately determined from the settlement of soil around a vertical pipe housing one of the array seismographs. The seismic compression at the site was ~10-20 cm. The profile at the site was well characterized by in-situ tests and laboratory tests performed on samples from the site, which allows seismic compression models to be calibrated. The study presented herein compares the predictions of the simplified and non-simplified forms of the expanded Byrne model. The predictions are in good accord with field observations, but the slight under-prediction by the non-simplified model may relate to estimated soil properties, assumed orientation of the ground motions and accounting for multidirectional shaking, and/or the numerical site response analyses used to compute the variation of the shear strains during shaking at depth in the soil profile.

Keywords: seismic compression; geotechnical earthquake engineering; unsaturated sand; shake down

4b-0048

17WCE

Sendal, Japan

2020

17th World Conference on Earthquake Engineering, 17WCEE Sendai, Japan - September 13th to 18th 2020

## 1. Introduction

Seismic compression is the accrual of contractive volumetric strain in unsaturated or partially saturated sandy soils during earthquake shaking (i.e., vibration-induced settlement) (Stewart et al. [1]). Seismic compression has occurred in several earthquakes and can significantly distress overlying and nearby structures. Adopting the terminology used for liquefaction triggering procedures, with slight modification, seismic compression evaluation procedures can be broadly classified as "simplified" and "non-simplified." In the context used herein, simplified approaches use relatively simple ground motion parameterization to characterize the seismic demand (e.g., effective shear strain,  $\gamma_{eff}$ , and number of equivalent strain cycles,  $n_{eq\gamma}$ ), while non-simplified procedures use more detailed characterization of seismic demand (e.g., shear strain,  $\gamma$ , time histories computed using numerical site response analyses).

The objective of the study presented herein is to use the simplified and non-simplified forms of the expanded Byrne [2] cyclic shear-volume strain coupling model to analyze a well-documented case history from the 2007, M<sub>w</sub>6.6 Niigata-ken Chuetsu-oki earthquake. The magnitudes of the predicted seismic compression using the two forms are compared to post-event field observations and discussed.

# 2. Expanded Byrne Model

Byrne [2] proposed the following variant of the Martin et al. [3] cyclic shear-volume strain coupling non-simplified model to estimate volumetric strains in dry sands:

$$\varepsilon_{\nu} = \sum_{i} \left( \Delta \varepsilon_{\nu, 1/2} \right)_{i} \tag{1a}$$

where  $\varepsilon_v$  = accumulated volumetric strain in percent at the end of loading; and  $(\Delta \varepsilon_{v,1/2})_i$  = increment in volumetric strain in percent at the end of the  $i^{th}$  half-shear strain cycle of loading having an amplitude  $\gamma_i$ . For earthquake loading,  $\gamma_i$  is typically taken as the peak shear strain between two zero crossings in the shear strain time history (e.g., Green and Terri [4]).  $(\Delta \varepsilon_{v,1/2})_i$  is computed as:

$$\left(\Delta \varepsilon_{v,1/2}\right)_{i} = 0.5 \cdot (\gamma_{i} - \gamma_{tv}) \cdot C_{1} \cdot exp\left[-C_{2} \frac{\varepsilon_{vi}}{(\gamma_{i} - \gamma_{tv})}\right] \tag{1b}$$

where  $C_1$  and  $C_2$  are material-specific calibration parameters;  $\varepsilon_{vi}$  is the volumetric strain in percent at the beginning of the  $i^{th}$  load increment;  $\gamma_{tv}$  = threshold shear strain in percent; and  $\gamma_i$  is in percent. Based on the analysis of the laboratory data for Crystal Silica Sand No. 2 from Silver and Seed [5] and Seed and Silver [6], Byrne [2] provided expressions to estimate  $C_1$  and  $C_2$ :

$$C_1 = 7,600 \cdot Dr^{-2.5} \tag{2a}$$

$$C_2 = \frac{0.4}{C_1}$$
 (2b)

where Dr is the relative density of the sand in percent.

As detailed in the Jiang et al. [7], the Byrne [2] model can be written in the alternative form:

$$\varepsilon_{v_i} = -\ln(\prod_i t_i) \cdot \frac{(\gamma_i - \gamma_{tv})}{c_2} \tag{3a}$$

4b-0048

17WCE

Sendai, Japan
2020

17th World Conference on Earthquake Engineering, 17WCEE Sendai, Japan - September 13th to 18th 2020

where:

$$t_{i} = \begin{cases} e^{-0.5 \cdot C_{1} \cdot C_{2}} & \text{if } i = 1\\ (t_{i-1})^{t_{i-1}} & \text{if } i > 1 \end{cases}$$
(3b)

and  $\varepsilon_{vi}$  is in percent at the end of the  $i^{th}$  load increment having amplitude  $\gamma_i$ , and both  $\gamma_i$  and  $\gamma_{tv}$  are in percent. If the seismic demand is expressed in terms of  $\gamma_{eff}$  and  $n_{eq\gamma}$ , Eq. (3) can be written in simplified form:

$$\varepsilon_{v} = -\ln\left(\prod_{i=1}^{2 \cdot n_{eq\gamma}} t_{i}\right) \cdot \frac{(\gamma_{eff} - \gamma_{tv})}{c_{2}} \tag{4}$$

where  $\varepsilon_v$  is the volumetric strain at the end of shaking,  $\gamma_{eff}$  is typically taken as 0.65 the peak shear strain at the depth of interest (e.g., Dobry et al. [8]), and  $n_{eq\gamma}$  is estimated using empirical correlations (e.g., Green and Lee [9]; Lee and Green [10]).

Comparison of Eq. (4) with laboratory data and with simplified equations proposed by Duku et al. [11] and Yee et al. [12], dictates that the Byrne model be expanded. Specifically, the simplified form of the Byrne model can be expanded to:

$$\varepsilon_{v} = -\ln\left(\prod_{i=1}^{2 \cdot n_{eq\gamma}} t_{i}\right) \cdot \frac{\left(\gamma_{eff} - \gamma_{tv}\right)^{C_{3}}}{c_{2}} \tag{5}$$

and to:

$$\left(\Delta \varepsilon_{v,1/2}\right)_i = 0.5 \cdot (\gamma_i - \gamma_{tv})^{C_3} \cdot C_1 \cdot exp\left[-C_2 \frac{\varepsilon_{vi}}{(\gamma_i - \gamma_{tv})^{C_3}}\right] \tag{6}$$

for the non-simplified form.

The calibration coefficients for Eq. (5) (i.e., C1, C2, and C3) are the same as those for Eq. (6). Using the data and the simplified models from Duku et al. [11] and Yee et al. [12] for clean sands and non-plastic to moderately plastic silty sands/sandy silts (i.e., Plasticity Index,  $PI \le 10$ ), with Fines Content (FC) ranging from 0 to 60%:

$$C_1 = \frac{1}{F_P(\gamma)} \cdot K_{FC} \cdot K_S \cdot K_{\sigma,\varepsilon} \cdot a_{1 atm}$$
 (7a)

$$F_P(\gamma) = \begin{cases} 2.8001 & \text{for clean sands} \\ 2.149 \cdot \gamma^{-0.2343} + 4.337 \cdot e^{-66.56\gamma} & \text{for silty sands/sandy silts} \end{cases}$$
 (7b)

$$K_{FC} = \frac{a_{FC}}{a_{FC=0}} = \begin{cases} 1 & \text{if} & 0 \le FC \le 10\% \\ e^{-0.042 \cdot (FC-10)} & \text{if} & 10\% < FC < \sim 35\% \\ 0.35 & \text{if} & FC \ge \sim 35\% \end{cases}$$
(7c)

4b-0048

17WCE

Sendal, Ignam

2020

17th World Conference on Earthquake Engineering, 17WCEE Sendai, Japan - September 13th to 18th 2020

$$K_{S} = \frac{a_{S}}{a_{S=0}} = \begin{cases} -0.017 \cdot S + 1 & \text{if } S < 30\% \\ 0.5 & \text{if } 30\% \le S < 50\% \\ 0.05 \cdot S - 2 & \text{if } 50\% \le S < 60\% \\ 1 & \text{if } S \ge 60\% \end{cases}$$
(7d)

$$K_{\sigma,\varepsilon} = \frac{a_{\sigma}}{a_{1 atm}} = \left(\frac{\sigma_{v}'}{P_{a}}\right)^{-0.29} \tag{7e}$$

$$a_{1 atm} = 5.38 \cdot exp(-0.023 \cdot Dr)$$
 (7f)

$$C_2 = \frac{P(\gamma)}{c_1} \tag{7g}$$

$$P(\gamma) = \begin{cases} 1 & \text{for clean sands} \\ e^{0.405} \cdot (\gamma - \gamma_{tv})^{0.3291} & \text{for silty sands/sandy silts} \end{cases}$$
 (7h)

$$C_3 = 1.2 \tag{7i}$$

where Dr, FC, Saturation (S),  $\gamma$ , and  $\gamma_{tv}$  are in percent.

# 3. KKNPP Case History

## 3.1 Background

The main shock of the  $M_w6.6$  Niigata-ken Chuetsu-oki, Japan, earthquake occurred on 16 July 2007. The event affected an  $\sim 100$ -km-wide area along the coastal regions of southwestern Niigata prefecture and triggered ground failures as far as the Unouma Hills, located in central Niigata approximately 50 km from the shore (Kayen et al. [13]). Of specific interest to this study is the seismic compression that occurred during this event at the Kashiwazaki-Kariwa Nuclear Power Plant (KKNPP) site (Yee et al. [14]). What makes this case history of particular value is that the motions at the site were recorded by a free-field downhole array (Service Hall Array, SHA) and the magnitude of the seismic compression was accurately determined from the settlement of soil around a vertical pipe housing one of the array seismographs. The geometric mean of the peak accelerations at bedrock and the ground surface were  $\sim 0.55g$  and  $\sim 0.4g$ , respectively, indicating nonlinear site response of the soil column. The seismic compression at the site was  $\sim 10-20$  cm.

Yee et al. [14] performed a detailed site investigation and determined that the profile at the strong motion array consists of ~70 m of medium-dense sands overlying clayey bedrock and that the ground water table (gwt) is at a depth of ~45 m. Suspension logging and Standard Penetration Tests (SPT) with energy measurements were performed at the site, with the former providing small-strain shear and compression wave velocities (i.e., Vs and Vp, respectively). Additionally, laboratory tests were performed on disturbed and undisturbed samples to classify the soil, to determine index properties and shear strength of the soil, and to develop modulus reduction and damping (MRD) curves. The geologic log and instrument locations for the SHA site are shown in Fig. 1. Also, shown in this figure are the results SPT and suspension logging geophysical testing and some of their interpretation.

4b-0048

Nake it safer

17WCEE

Scrudal, Japan

2020

17th World Conference on Earthquake Engineering, 17WCEE
Sendai, Japan - September 13th to 18th 2020

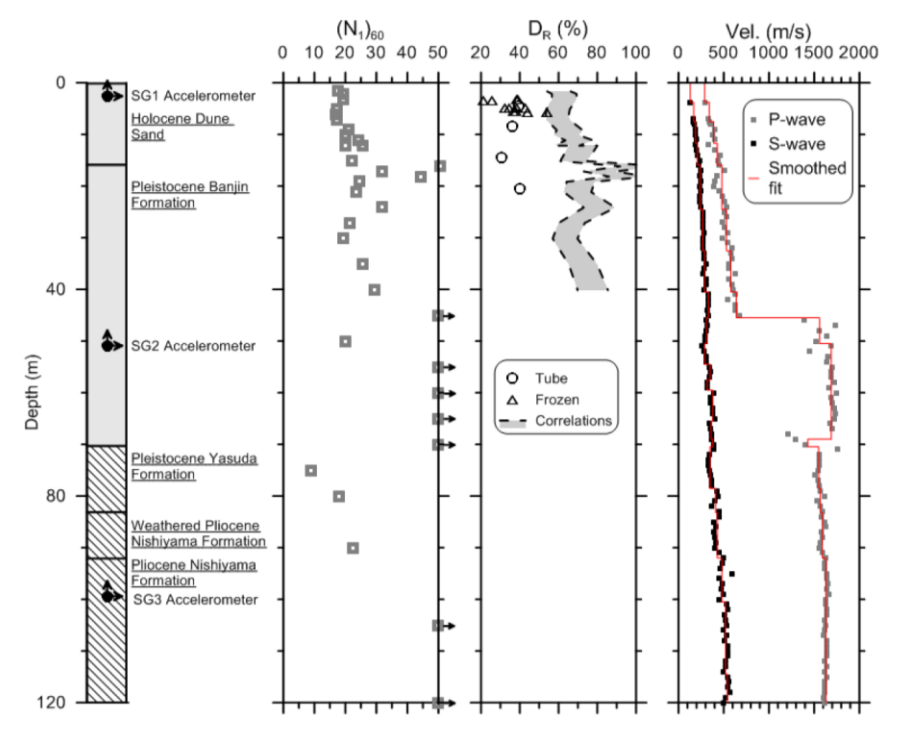


Fig. 1 – Geologic log for the SHA site including instrument locations and data SPT and suspension logging geophysical testing (Yee et al. [14])

## 3.2 Seismic compression

Yee et al. [14] performed a series of drained cyclic simple shear tests on samples from the KKNPP site and the results are used herein to develop relationships for the calibration parameters (i.e.,  $C_1$ ,  $C_2$ , and  $C_3$ ) for the simplified and non-simplified forms of the expanded Byrne model (i.e., Eqs. (5) and (6)) for  $Dr \approx 35\%$  and 60%:

$$C_1 = K_{\sigma,\varepsilon} \cdot 1.28 \cdot e^{-0.019 \cdot Dr} \tag{8a}$$

$$C_2 = \frac{0.7864}{c_1} \tag{8b}$$

$$C_3 = 1.2$$
 (8c)

where Dr is in percent. Additionally, Yee et al. [14] determined that  $\gamma_{tv}$  for the soil is ~0.03%. Dr for the soil is estimated using the relationship (Fig. 1):

$$Dr = 100 \cdot \sqrt{\frac{N_{1,60}}{c_d}} \tag{9}$$

where  $N_{1,60}$  is the corrected SPT blow count,  $C_d$  is a soil-specific parameter, and Dr is in percent. Per Skempton [15],  $C_d$  was assumed to be 55 (natural deposit of fine sand).

The Menq [16] modulus reduction and damping (MRD) curves are used to model the sandy soil above the gwt, with the Yee et al. [17] strength-adjustment applied and a minimum damping of 5% used. To



17th World Conference on Earthquake Engineering, 17WCEE Sendai, Japan - September 13th to 18th 2020

account for the influence of effective confining stress, the reference strain ( $\gamma_r$ ) used in the Menq [16] modulus reduction curves (i.e., curves of  $(G/G_{max})_{\gamma eff}$  vs.  $\gamma_{eff}$ ) were adjusted using:

$$\gamma_r = \gamma_{r,1} \cdot \left(\frac{\sigma_o'}{P_a}\right)^n \tag{10}$$

where  $\sigma'_{o}$  is the mean effective confining stress; Pa is atmospheric pressure in the same units as  $\sigma'_{o}$ ;  $\gamma_{r,1}$  is the reference strain for  $\sigma'_{o} = 1$  atm; and n is an empirical soil-specific factor. Based on the MRD test data for sandy soils above the gwt from the KKNPP site,  $\gamma_{r,1} = 0.0904$  and n = 0.4345 (Yee et al. [17]). No samples from below the gwt from the site were tested, and it is assumed that the  $\gamma_{r,1}$  and n values proposed by Menq [16] apply to sandy soils below the gwt:  $\gamma_{r,1} = 0.0684$  and n = 0.4345. The Darendeli [18] MRD curves were used for the relatively plastic soils and rock materials below 70 m. To compute  $\sigma'_{o}$ , the total unit weights ( $\gamma_{t}$ ) of the soil listed in Table 1 were assumed and used in conjunction with at rest lateral earth pressures for the various strata listed in Yee et al. [14].

Table 1 – Assumed soil types and unit weights used in analysis (Motamed et al. [19])

Depth range (m)	Soil type	Total unit weight, $\gamma_t$ (kN/m <sup>3</sup> )
0-4	Sand	16
4-45	Sand	17.75
45-70	Sand	20.8
70-99.4	Clay	20.8

As discussed next, the simplified and non-simplified forms of the expanded Byrne model were used in conjunction with site-specific data to predict the settlement due to seismic compression at the KKNPP site. The total settlement at the ground surface  $(S_T)$  at the site is related to the  $\varepsilon_v$  values for each layer as:

$$S_T = \sum_j \varepsilon_{v_j} \cdot \Delta z_j \tag{11}$$

where  $\varepsilon_{vj}$  is the volumetric strain in the  $j^{th}$  layer; and  $\Delta z_j$  is the thickness of the  $j^{th}$  layer.

# 3.2.1 Simplified analysis

As stated in the Introduction, the distinction between simplified and non-simplified approaches for predicting the magnitude of seismic compression relates to the how the ground motions are characterized. For simplified analyses, the ground motions are characterized by the amplitude of the effective shear strain ( $\gamma_{eff}$ ) and the number of equivalent strain cycles ( $n_{eq\gamma}$ ).  $\gamma_{eff}$  is typically defined as 0.65 of the amplitude of the peak shear strain induced in the soil layer during the earthquake shaking.  $\gamma_{eff}$  can estimated using an expression that was derived similarly to the one used to compute Cyclic Stress Ratio (CSR) in simplified liquefaction evaluation procedures (Dobry et al. [8]):

$$\gamma_{eff} = \frac{\tau_{av}}{G_{\gamma_{eff}}} \approx \frac{0.65 \frac{a_{max}}{g} \cdot \sigma_v \cdot r_d}{G_{max} \cdot \left(\frac{G}{G_{max}}\right)_{\gamma_{eff}}}$$
(12)

4b-0048

Nake it safer

17WCEE

Sendai, Japan

2020

17th World Conference on Earthquake Engineering, 17WCEE
Sendai, Japan - September 13th to 18th 2020

where:  $\tau_{av}$  is the average cyclic stress imposed on the soil at given depth in the profile over the duration of strong ground shaking;  $G_{\gamma eff}$  is the secant shear modulus corresponding to  $\gamma_{eff}$  and having the same units as  $\tau_{av}$ ;  $a_{max}$  is the peak horizontal ground acceleration at the surface of the soil profile; g is the acceleration due to gravity in the same units as  $a_{max}$ ;  $\sigma_v$  is the total vertical stress at the depth of interest;  $r_d$  is the dimensionless depth-stress reduction factor that accounts for the non-linear response of the profile during earthquake shaking;  $G_{max}$  is the small strain ( $\gamma < 10^{-40}$ %) secant shear modulus in the same units as  $\sigma_v$ ; and  $(G/G_{max})_{\gamma eff}$  is the ratio of  $G_{\gamma eff}$  and  $G_{max}$ . Because  $\gamma_{eff}$  is a function of a  $G_{\gamma eff}$  (or  $G_{max} \cdot (G/G_{max})_{\gamma eff}$ ), which in turn is a function of  $\gamma_{eff}$ , Eq. (12) needs to be solved iteratively or by using the chart solution proposed by Tokimatsu and Seed [20], or similar ones.

Eq. (12) was solved iteratively using the modulus reduction curves discussed above and  $a_{max} = 0.4g$  (i.e., geometric mean of the recorded peak accelerations at ground surface). The  $r_d$  relationship proposed by Idriss [21] was used. Although Lasley et al. [22] shows that this relationship generally predicts too rigid of profile response for liquefaction triggering analyses, the profiles for seismic compression analyses tend to be stiffer than sites evaluated for liquefaction due to deeper gwt (or higher effective confining stresses). As a result, it is recommended that the Idriss [21]  $r_d$  relationship be used to compute  $\gamma_{eff}$  in seismic compression analyses.

Fig. 2 is a plot of the  $\gamma_{eff}$  computed using Eq. (12). For comparison,  $\gamma_{eff}$  was also computed from the shear strain time histories from the equivalent linear (EQL) numerical site response analyses, discussed subsequently. For these latter values,  $\gamma_{eff}$  was computed as 0.65 times the geometric mean of the peak shear strains in each layer resulting from the EQL analyses using the EW and NS motions. As may be observed from Fig. 2,  $\gamma_{eff}$  computed using Eq. (12) have a similar trend with depth as those from the EQL analyses, but are slightly larger in magnitude for most depths.

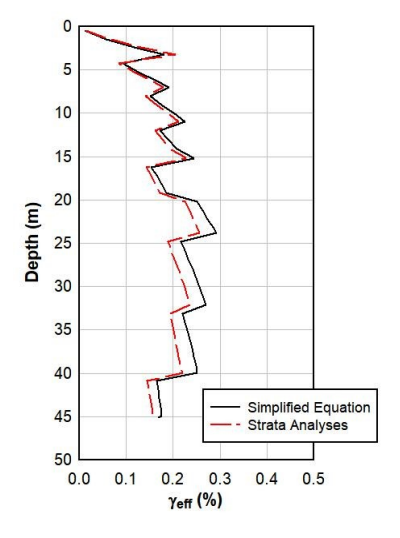


Fig. 2 –  $\gamma_{eff}$  computed using the Eq. (12) and from the EQL analyses

The relationship proposed by Lee and Green [10] for shallow crustal events in active tectonic regimes was used to compute  $n_{eq\gamma}$ :

$$ln(n_{eq\gamma}) = exp(-0.0099 \cdot z) + 0.67 \cdot R_{rup}^{0.21} + 0.28 \cdot M_w - 1.79$$
(13)

where z is depth below the ground surface in m;  $R_{\text{rup}}$  is the closest distance to the fault rupture plane (km); and  $M_w$  is moment magnitude. Yee et al. [14] give  $R_{\text{rup}} = 16$  km. This relationship is preferred over others because it was specifically developed for computing the  $n_{\text{eq}\gamma}$  for seismic compression analyses. Its use is in contrast to the common practice of using relationships for number of equivalent shear stress cycles ( $n_{\text{eq}\tau}$ )

4b-0048

Make it sufer

17WCEE

Sendal, Japan

2020

17th World Conference on Earthquake Engineering, 17WCEE Sendai, Japan - September 13th to 18th 2020

developed for liquefaction triggering analyses in seismic compression analyses, which fails to recognize the potential differences between  $n_{eq\gamma}$  and  $n_{eq\tau}$  (see details in Green and Terri [4]). Fig. 3 shows a plot of the computed  $n_{eq\gamma}$  vs. depth for the event.

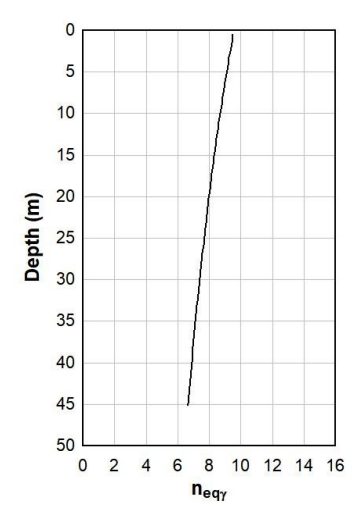


Fig.  $3 - n_{eq\gamma}$  as a function of depth computed using the relationship by Lee and Green [10] for shallow crustal events in active tectonic regimes

The observed surface settlement at the KKNPP likely reflects the seismic compression that occurred in the unsaturated or partially saturated sandy soil above the gwt and settlement that occurred in the saturated sandy soil below the gwt (the soil below the gwt is assumed to be saturated based on Vp measurements of ~1500 m/s shown in Fig. 1). Pyke [23] provides some guidance on how to compute the settlement of the saturated sandy soil subjected to earthquake shaking: "While not checked experimentally, it was assumed in the studies reported by Martin et al. [3] and Seed et al. [24] that the latent settlement generated in a fully saturated sand was equal to the actual settlement of a dry sand up to the point of initial liquefaction, and this assumption appeared to yield good results. Once initial liquefaction (or 100 percent excess pore pressure ratio) is reached, larger latent settlements will be generated." None of the ground motion recordings from the SHA array exhibited characteristics of the ground softening due to higher levels excess pore pressure generation (e.g., Wotherspoon et al. [25]). Accordingly, following the guidance in Pyke [23], the settlement of the sandy soil both above and below the gwt at the KKNPP site was evaluated using the using the expanded Byrne model.

In a detailed, but somewhat limited, laboratory study, Pyke et al. [26] examined the influence of multidirectional shaking on seismic compression. They found that the direct addition of the settlements in the soil resulting from being subjected to each horizontal component of motion separately is appropriate. They also found that vertical motions can increase the seismic compression due to horizontal motions by 20% to 50% for Peak Ground Accelerations (PGAs) ranging from 0.15g to 0.3g, respectively, when acting in combination with horizontal motions. This would imply that the seismic compression computed using the sum of the seismic compression computed using the PGAs for the EW and NS surface motions at the KKNPP site should be increased by  $\sim$ 50% because the effective peak vertical acceleration at the site is  $\sim$ 0.4g (Yee et al. [14]).

The predicted settlement due to seismic compression using the simplified expanded Byrne model is  $\sim$ 16.4 cm.

## 3.2.2 Non-Simplified analysis

The main advantage of non-simplified procedures is that they allow for the use of a more detailed characterization of the seismic demand at all depths in the profile. Most notably, this allows the variation in

4b-0048

Nake it safer

17WCEE
Sendal, Japan
2020

17th World Conference on Earthquake Engineering, 17WCEE Sendai, Japan - September 13th to 18th 2020

induced shear strains over the duration of shaking to be accounted for, which influences the resulting volumetric strain in materials that exhibit load-dependent, interaction fatigue behavior (e.g., Lasley et al. [27]). Because performing site response analyses needed for implementing non-simplified procedures has become state-of-practice in many regions of the world, non-simplified procedures are a viable option for more accurately predicting seismic compression in today's practice. The disadvantage of using non-simplified procedures is that they require more effort to implement, to include a more-detailed characterization of the site being analyzed, selection of appropriate input ground motions for the site response analysis, and the complexity of implementing the procedure itself.

For the study presented herein, one-dimensional EQL site response analyses were performed for the site using the software Strata (Kottke and Rathje [28]) following the modeling details in Yee et al. [14], [17]. The unprocessed ground motions recorded by the SHA array were obtained from the Tokyo Electric Power Company (TEPCO) and were processed following the procedures detailed in Boore [29], and Boore and Bommer [30]. The horizontal motions were oriented in the EW and NS directions, and those corresponding to a depth of 99.4 m were specified as "with-in" input motions in the EQL analyses. The motions are shown in Fig. 4.

To validate the EQL model, computed and recorded motions were compared at depths of 2.4 m and 50.8 m. The horizontal PGAs for the recorded and computed motions were in good agreement, as were the response spectra (Jiang et al. [7]). Additionally, the validity of the one-dimensional profile response assumption was assessed using the criteria detailed in Toa and Rathje [31] and shown to be valid. Accordingly, the EQL model was used to compute the shear strain time histories at the center of each of the model layers that are susceptible to seismic compression. These time histories were used in conjunction with the non-simplified form of the expanded Byrne model to compute the  $\epsilon_v$  in each layer and the overall settlement at the site due to seismic compression. The predicted settlement due to seismic compression using the simplified expanded Byrne model is ~9.75 cm, which includes the influence of all three components of motion.

#### 4. Discussion

The predicted settlements using the simplified and non-simplified forms of the expanded Byrne model are in general accord with post-earthquake field observations at the KKNPP site (i.e.,  $\sim 16.4$  cm &  $\sim 9.75$  cm vs. 10 - 20 cm). Note that although the simplified form of the expanded Byrne model is predicting settlements that are within the range of field observations and the non-simplified form's predictions are slightly less than the observed range, this should not be interpreted as the simplified procedure being a superior or more accurate approach. It is doubtful that the simplified form will always predict more accurate settlements (or even larger settlements) than the non-simplified form. Rather, the non-simplified procedure should be viewed as providing more accurate estimates of the predicted seismic compression if the required inputs and model assumptions used in the analyses are appropriate.

Given that the KKNPP SHA site was very well characterized, the site response model was validated and the motions used in modeling were those that were recorded at the site, and the seismic compression model was calibrated using soil from the site, potential reasons for the slight under-prediction of the non-simplified model need to be considered. These include the estimated Dr and  $\gamma_{tv}$  of the soil, orientation of the ground motions used in the analyses, how multidirectional shaking is being accounted for, influence of soil fabric, and EQL vs. non-linear (NL) numerical site response analyses to compute the shear strain time histories at depth in the soil profile. These factors are discussed in detail in Jiang et al. [7], and although additional studies are needed to further explore these issues, some of their findings are:

• Estimation of Dr and  $\gamma_{tv}$ , and ground motion orientation, individually, have moderate to significant influences on the computed magnitude of seismic compression, but in combination they can have significant influence; and

4b-0048

Make it safer

17WCEB
Sendai, Japan

2020

17th World Conference on Earthquake Engineering, 17WCEE Sendai, Japan - September 13th to 18th 2020

• How multidirectional shaking is accounted for has a significant influence on the computed magnitude of seismic compression.

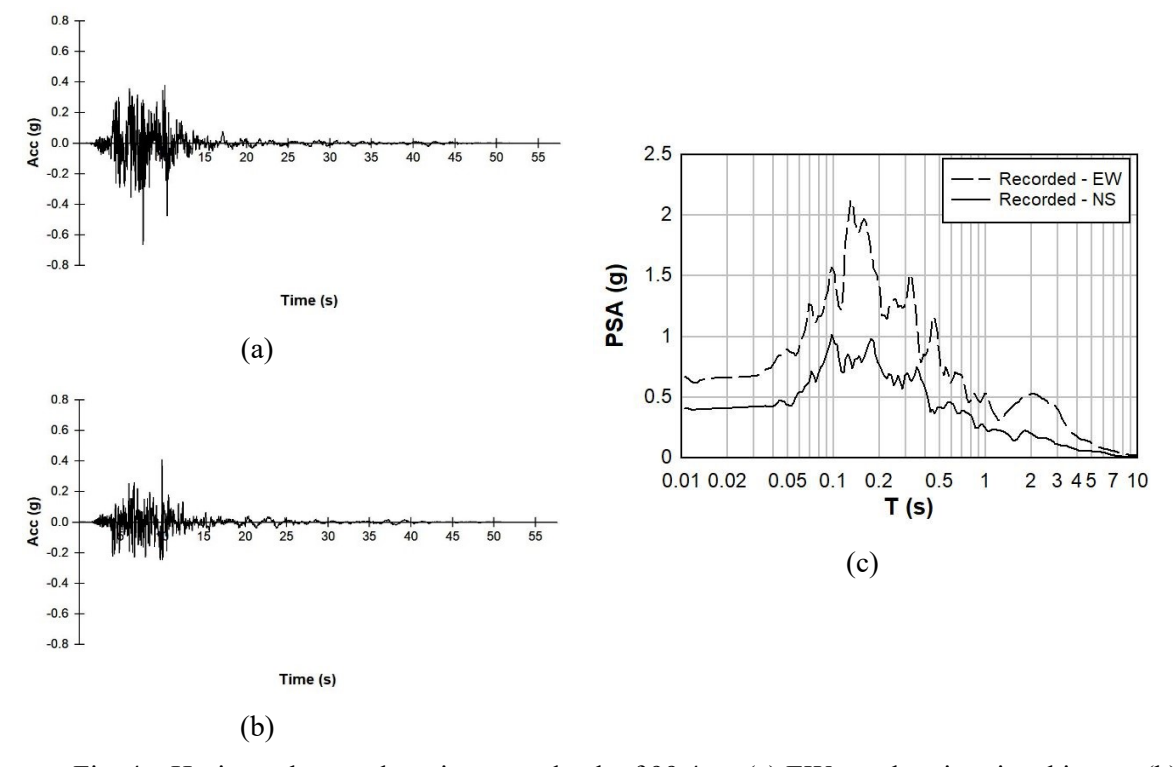


Fig. 4 – Horizontal ground motions at a depth of 99.4 m: (a) EW acceleration time history; (b) NS acceleration time history; and (c) corresponding pseudo spectral accelerations

## 5. Conclusion

Together the simplified and non-simplified forms of the expanded Byrne model provide a versatile approach for evaluating seismic compression that is scalable based on available data and the importance of the project. Both forms of the model use the same calibration parameters, which have been developed herein for clean sands and non-plastic to moderately plastic ( $PI \le 10$ ) silty sands/sandy silts using the extensive laboratory data performed by researchers at the University of California at Los Angeles. The non-simplified form is relatively easy to implement and thus, overcomes the complexity issues with implementing other non-simplified models (e.g., Lasley et al. [27]; Yee and Steward [32]).

Both the simplified and non-simplified forms of the expanded Byrne models were used to evaluate seismic compression at the KKNPP SHA site during the main shock of the 2007,  $M_w6.6$  Niigata-ken Chuetsu-oki, Japan, earthquake. The predicted settlements are in general accord with post-earthquake field observations at the KKNPP site (i.e., simplified: ~16.4 cm & non-simplified: ~9.75 cm vs. field observations: 10-20 cm). Although the simplified form of the expanded Byrne model is predicting settlements that are within the range of field observations and the non-simplified form predicts settlements that are slightly less than the observed range, this should not be interpreted as the simplified procedure being a superior or more accurate approach. It is doubtful that the simplified form will always predict more accurate settlements (or even larger settlements) than the non-simplified form. Rather, the non-simplified procedure should be viewed as providing more accurate estimates of the predicted seismic compression if the required inputs and model assumptions used in the analyses are appropriate. Although additional studies are needed to further explore the factors resulting in the slight under-prediction of the non-simplified form of the model, likely reasons related to:

4b-0048

17WCE
Sendal, Japan
2020

17th World Conference on Earthquake Engineering, 17WCEE
Sendai, Japan - September 13th to 18th 2020

- Estimation of Dr and γ<sub>tv</sub>, and ground motion orientation, individually, have moderate to significant influences on the computed magnitude of seismic compression, but in combination they can have significant influence; and
- How multidirectional shaking is accounted for has a significant influence on the computed magnitude of seismic compression.

# 6. Acknowledgements

This study is based on work supported by the US Army Engineer Research and Development Center (ERDC) Grant W912HZ-13-C-0035 and U.S. National Science Foundation (NSF) Grants CMMI-1435494, CMMI-1724575, and CMMI-1825189. The authors gratefully acknowledge this funding. Additionally, the authors greatly appreciate the help from Dr. Oliver-Denzil Taylor, and Professors Jonathan Stewart and Ramin Motamed regarding the KKNPP case history and from Mr. Mahdi Bahrampouri in processing the KKNPP ground motions. The ground motion data used in this study belongs Tokyo Electric Power Company, and the distribution license of the data belongs to Japan Association for Earthquake Engineering (JAEE). Finally, any opinions, findings, and conclusions or recommendations expressed in this paper are those of the authors and do not necessarily reflect the views of ERDC, NSF, or JAEE or those that have provided help on this study.

#### 7. References

- [1] Stewart JP, Smith PM, Whang DH, Bray J.D. (2004): Seismic compression of two compacted earth fills shaken by the 1994 Northridge earthquake. *J. Geotech. Geoenviron. Eng.*, **130** (5), 461-476.
- [2] Byrne P (1991): A cyclic shear-volume coupling and pore pressure model for sand. *Proc., 2nd Int. Conf. on Recent Advances in Geotechnical Earthquake Engineering and Soil Dynamics*, Missouri Univ. of Science and Technology, Rolla, MO, 47–55.
- [3] Martin GR, Finn WDL, Seed HB (1975): Fundamentals of liquefaction under cyclic loading. *J. Geotech. Eng. Div.*, **101** (GT5), 423–438.
- [4] Green RA, Terri GA (2005): Number of equivalent cycles concept for liquefaction evaluations—Revisited. *J. Geotech. Geoenviron. Eng.*, **131** (4), 477–488.
- [5] Silver ML, Seed HB (1971): Volume changes in sands during cyclic loading. *J. Soil Mech. Found. Div.*, **97** (SM9), 1171–1182.
- [6] Seed HB, Silver ML (1972): Settlement of dry sands during earthquakes. J. Soil Mech. Found. Div., 98 (SM4), 381–397.
- [7] Jiang Y, Green RA, Taylor O-D (2020): Expanded Byrne Model for Evaluating Seismic Compression. *Earthquake Spectra*, (*in review*).
- [8] Dobry R, Ladd RS, Yokel FY, Chung RM, Powell D (1982): *Prediction of Pore Water Pressure Buildup and Liquefaction of Sands During Earthquakes by the Cyclic Strain Methods*. Building Science Series 138, National Bureau of Standards, U.S. Department of Commerce, U.S. Government Printing Office, Washington, D.C.
- [9] Green RA, Lee J (2006): Computation of number of equivalent strain cycles: A theoretical framework. *Geomechanics II: Testing, modeling, and simulation*, P. V. Lade and T. Nakai, eds., ASCE, Reston, VA, 471–487.
- [10] Lee J, Green RA (2017): Number of Equivalent Strain Cycles for Active Tectonic and Stable Continental Regions. *Proc.* 19<sup>th</sup> Intern. Conf. on Soil Mechanics and Geotechnical Engineering, Seoul, Korea, 17-22 September.
- [11] Duku PM, Stewart JP, Whang DH, Yee E (2008): Volumetric strains of clean sands subject to cyclic loads. *J. Geotech. Geoenviron. Eng.*, **134** (8), 1073-1085.
- [12] Yee E, Duku PM, Stewart JP (2014): Cyclic volumetric strain behavior of sands with fines of low plasticity. *J. Geotech. Geoenviron. Eng.*, 10.1061/(ASCE)GT.1943-5606.0001041, 04013042.

4b-0048

17WCE

Sendal, Japan
2020

17<sup>th</sup> World Conference on Earthquake Engineering, 17WCEE Sendai, Japan - September 13th to 18th 2020

- [13] Kayen R, Brandenberg SJ, Collins BD, Dickenson S, Ashford S, Kawamata Y, Tanaka Y, Koumoto H, Abrahamson N, Cluff L, Tokimatsu K (2009): Geoengineering and seismological aspects of the Niigata-ken Chuetsu-oki earthquake of 16 July 2007. *Earthquake Spectra*, **25** (4), 777–802.
- [14] Yee E, Stewart JP, Tokimatsu K (2011): Nonlinear site response and seismic compression at vertical array strongly shaken by 2007 Niigata-ken Chuetsu-oki earthquake. *Rep. No. 2011/107*, Pacific Earthquake Engineering Research Center, Univ. of California, Berkeley, CA.
- [15] Skempton AW (1986): Standard penetration test procedures and the effects in sands of overburden pressure, relative density, particle size, aging, and overconsolidation. *Geotechnique*, **36** (3), 425-447.
- [16] Menq FY (2003): Dynamic properties of sandy and gravelly soils. *Ph.D. Dissertation*, Dept. of Civil Eng., Univ. of Texas, Austin, TX.
- [17] Yee E, Stewart JP, Tokimatsu K (2013): Elastic and large-strain nonlinear seismic site response from analysis of vertical array recordings. *J. Geotech. Geoenviron. Eng.*, 10.1061/(ASCE)GT.1943-5606.0000900, 1789–1801.
- [18] Darendeli M (2001): Development of a new family of normalized modulus reduction and material damping curves. *Ph.D. Dissertation*, Dept. of Civil Eng., Univ. of Texas, Austin, TX.
- [19] Motamed R, Stanton K, Almufti I, Ellison K, Willford M (2016): Improved approach for modeling nonlinear site response of highly strained soils: Case study of Service Hall Array in Japan. *Earthquake Spectra*, **32** (2), 1055-1074.
- [20] Tokimatsu K, Seed HB (1987): Evaluation of settlements in sand due to earthquake shaking. *J. of Geotech. Engrg.*, **113** (8), 861-878.
- [21] Idriss IM (1999): An update to the Seed-Idriss simplified procedure for evaluating liquefaction potential. *Proc.*, *TRB Workshop on New Approaches to Liquefaction Analysis*, U.S. Dept. of Transportation, Federal Highway Administration, Washington, DC.
- [22] Lasley S, Green RA, Rodriguez-Marek A (2016b): A New Stress Reduction Coefficient Relationship for Liquefaction Triggering Analyses. Technical Note, *J. Geotech. Geoenviron. Eng.*, **142** (11), 06016013-1.
- [23] Pyke R (2019): Improved Analyses of Earthquake-Induced Liquefaction and Settlement. *Proc.* 7<sup>th</sup> Intern. Conf. Earthquake Geotechnical Engineering (7ICEGE), Rome, Italy, 17-20 June 2019.
- [24] Seed HB, Pyke R, Martin GR (1978): Effect of Multi-Directional Shaking on Pore Pressure Development in Sands. J. Geotech. Engrg. Div., 104 (GT1), 27-44.
- [25] Wotherspoon LM, Orense RP, Green RA, Bradley BA, Cox BR, Wood CM (2015): Assessment of liquefaction evaluation procedures and severity index frameworks at Christchurch strong motion stations. *Soil Dyn. Earthquake Engrg.*, **79** (Part B), 335–346.
- [26] Pyke R, Seed HB, Chan CK (1975): Settlement of sands under multidirectional shaking. *J. Geotech. Engrg.*, **101** (4), 379-398.
- [27] Lasley S, Green RA, Chen Q, Rodriguez-Marek A (2016a): Approach for Estimating Seismic Compression Using Site Response Analyses. *J. Geotech. Geoenviron. Eng.*, **142** (6), 04016015.
- [28] Kottke A, Rathje EM (2009): Technical Manual for Strata. *PEER 2008/10*, Pacific Earthquake Engineering Research Center, University of California at Berkeley, Berkeley, CA.
- [29] Boore DM (2005): On pads and filters: processing strong-motion data. Bull. of the Seis. Soc. of Am., 95, 745-750.
- [30] Boore BM, Bommer JJ (2005): Processing of strong-motion accelerograms: needs, options and consequences. *Soil Dyn. Earthquake Engrg.*, **25**, 93–115.
- [31] Toa Y, Rathje E (2019): Taxonomy for Evaluating the Site-Specific Applicability of One-Dimensional Ground Response Analysis. *Soil Dyn. Earthquake Engrg.*, **128**, 1–13.
- [32] Yee E, Stewart JP (2018): A comparison of alternative seismic compression procedures. *Geotechnical Earthquake Engineering and Soil Dynamics V: Seismic Hazard Analysis, Earthquake Ground Motions, and Regional-Scale Assessment*, GSP 291, ASCE, Reston, VA.